Alpha-Particle Stopping Cross Section of Solids from 0.3 to 2.0 MeV*

W. K. Lin, H. G. Olson, and D. Powers
Baylor University, Waco, Texas 76703
(Received 26 February 1973)

Stopping cross sections of α particles for 12 solid elements Se, Y, Zr, Nb, Mo, Sb, Te, La, Dy, Ta, W, and Au have been measured for $0.3 < E_a < 2.0$ MeV. Structure additional to that previously obtained was observed, in the periodic dependence of the stopping cross section on the atomic number of the stopping element. Good agreement in the periodic dependence of the structure was found when the experimental results were compared to theoretical calculations based on Lindhard's statistical approach, carried out by Rousseau, Chu, and Powers. The energy dependence of the stopping cross section was examined by fitting the experimental results to a three-parameter formula recently suggested by Brice. The usefulness of this formula in extrapolating the results to energy regions outside the measurements is investigated.

I. INTRODUCTION

The periodic dependence of the electronic stopping cross section S_e on the incident-ion atomic number Z_1 has been observed at low energies in atmospheric air and other gaseous media, in boron, carbon, and aluminum films, and in tungsten, silicon, and gold crystals. It has been concluded[1] that the positions of the oscillations are insensitive to the choice of Z_2 of the stopping element. S_e reaches its maxima around $Z_1 = 22$ and 41 and its minima around $Z_1 = 11$, 30, and 50.[2] The results and their significance in terms of the atomic shell effects are summarized by Cheshire and Poate.[1] A similar phenomenon, namely, the Z_2 oscillation of S_e, has also been seen in measurements of S_e for protons[3-5] and α particles.[5,6] This oscillation has its maxima around $Z_2 = 8$ and 22 and its minima around $Z_2 = 11$ and 29, and its periodic structure has been well reproduced in calculations of α-particle stopping cross sections, based on Lindhard's statistical approach, carried out by Rousseau, Chu, and Powers.[7,8] Hartree-Fock-Slater atomic wave functions were used in their calculations; additional maxima around $Z_2 = 40$, 57, and 90 and minima around $Z_2 = 46$ and 79 were predicted.

A charged particle loses its energy in the stopping medium by electronic and nuclear collisions. The portion of energy loss due to the electronic collisions, divided by the number of atoms in unit area, is often referred as the electronic stopping cross section of the medium. For larger Z_1, and with decreasing incident energy, the energy loss due to the nuclear collisions gradually becomes important. Experimentally it is more advantageous to study the periodic dependence of S_e on Z_2 rather than on Z_1, because for the former a smaller Z_1 (protons or α particles, for instance) can be used, and it is not necessary to subtract the nuclear contribution[9] in order to deduce the electronic stopping cross section. The present work was undertaken to measure S_e for α particles in the Z_2 region not covered in previous measurements,[5,6,10] and to see if the periodic structure also exists as predicted. The energy dependence of S_e was examined for each element by fitting the data to a three-parameter formula recently suggested by Brice.[11] One of the parameters, z, is introduced in the modification of Firsov's method, and the others, n and a, are used to enable a semiphenomenological extension to the high-velocity region. As Brice has pointed out that z is calculable from first principles, and a is shown to be a linear function of the stopping atomic size, therefore a systematic survey of these parameters for a series of elements may be interesting. The plausibility of using the extracted parameters to calculate S_e for other α-particle energies is investigated. This extrapolation is shown to be acceptable up to 10-MeV α-particle energy for those elements, with which there are measured or calculated values of S_e available for comparison. For other elements, for purposes of illustration, the extrapolated stopping cross sections were compared with the Bethe formula at higher energies.

II. EXPERIMENTAL METHOD

The experimental method consists of the elastic scattering of α particles either from a thick Ta backing onto which the stopping element has been evaporated, or directly from the film of the stopping element evaporated onto a thick Al backing. The former method has been described in detail in the measurements of α-particle stopping cross sections for lower-Z_2 elements by Chu and Powers.[6] It involves measuring the energies of α particles elastically scattered by Ta atoms on the front surface of a clean Ta blank and on that of another Ta blank onto which the target element has been evaporated. These two energies are denoted by E_{2B} and E_{2O}, respectively. For the target elements whose atomic weights are significantly greater than that of Al, the second method can be

used. E_{2B} and E_{2O} now correspond to the energies of α particles elastically scattered by the stopping atoms on the front and back surfaces of the target film. From the scattering kinematics, one has $E_{2B} = kE_\alpha$, where

$$k = \left(\frac{M_\alpha \cos\theta + (M^2 - M_\alpha^2 \sin^2\theta)^{1/2}}{M_\alpha + M} \right)^2 .$$

E_α and M_α are the incident energy and mass of the α particle. $\theta = 130°$ is the laboratory scattering angle, and M is the mass of the Ta atom or the vapor-deposited target atom, depending on whether the target is prepared on Ta or Al backing, respectively. The energy E_{2O}, expressed in terms of the energy losses ΔE_1 and ΔE_2 of the α particle before and after its scattering, is $k(E_\alpha - \Delta E_1) - \Delta E_2 = E_{2B} - (k\Delta E_1 + \Delta E_2)$. The difference $\Delta E = E_{2B} - E_{2O}$ is therefore related to the stopping cross section S_e by

$$\frac{\Delta E \cos\theta_1}{N\Delta x} = kS_e(\tilde{E}_1) + S_e(\tilde{E}_2).$$

$N\Delta x$ is the number of target atoms in unit area, and $\theta_1 = 25°$ is the angle between the incident beam and the normal to the target surface. ΔE_1 and ΔE_2 are evaluated at their corresponding mean energies $\tilde{E}_1$ and $\tilde{E}_2$ of the α particle before and after scattering. Since S_e is a smooth function of energy, it is sufficient to expand the right-hand side of this expression to the terms up to second derivative of S_e with respect to energy around an over-all mean energy E_x. The result is

$$\frac{\Delta E \cos\theta_1}{N\Delta x(1+k)} = S_e(E_x) + \frac{k}{2}\frac{d^2S_e}{dE_x^2}(E_\alpha - \delta - E_x)^2 , \qquad (1)$$

where $\delta = \Delta E/2(1+k)$. E_x is chosen to be equal to $(k\tilde{E}_1 + \tilde{E}_2)/(1+k)$, so that the first-derivative term vanishes. An approximate expression for E_x given by

$$E_x = \frac{E_{2B} + E_{2O}}{1+k} + \delta \frac{S_e(E_{2O}) - kS_e(E_\alpha)}{S_e(E_{2O}) + kS_e(E_\alpha)} , \qquad (2)$$

which includes corrections up to first-order smallness in both $\tilde{E}_1 - E_\alpha$ and $\tilde{E}_2 - E_{2O}$, was used in data reduction.

During target preparation, the backing blank of known weight was covered by a steel plate with a 2.85-cm^2 circular opening and placed 25 cm from the vapor source. The vacuum under which the evaporation by resistance heating or electron-beam bombardment were made, is better than 3×10^{-7} or 4×10^{-6} torr, respectively. After deposition within the above-mentioned area, the blank was weighed again. The increase in weight divided by the area gave the target thickness, and thus the number of atoms in unit target area, $N\Delta x$. Weighings were done by means of a Mettler M-5 microbalance, which has an accuracy up to 1.5 μg. Further information concerning each of the target elements used in this experiment is given in Table I. The Al blank used as a target backing has been shown,[12] from its x-ray diffractometer pattern, to be of polycrystalline structure; thus the possibility that the target element evaporated onto it forms a single crystal is small. The same situation is also expected for target elements prepared onto Ta backings, because no detectable difference was found between the stopping cross sections measured with Al and Ta backings. One would expect a negligible error from effects due to channeling in the target elements.

The magnetically analyzed He^+ beam from a 2-MV Van de Graaff accelerator was collimated to a 1.6-mm square before striking the target. The α particles elastically scattered at 130° were detected by a 100-μ surface-barrier counter, collimated by a 3×6-mm rectangular aperture 15 cm from the beam spot. The signal from the detector, through a preamplifier, linear amplifier, and a biased amplifier, was analyzed by a 50-MHz 256-channel analyzer. The target orientation was so fixed that the directions along both the incident and detected α particles were 25° with respect to the normal to the target surface. For lower bombarding energies, because of the increase in the Rutherford scattering cross section, the beam intensity (typically $\simeq$ 100 nA) was reduced to keep the possibility of pulse pileup in the analysis system negligibly small. Figure 1 shows the α-particle energy spectra obtained from bombardments on two selenium targets, one prepared on an Al backing and the other on a Ta backing. Spectrum (c) is from scattering of α particles by a clean Ta blank. The step indicated by C_{2B} corresponds to the α particles scattered from the front surface of the target, and its width is mainly due to the detector resolution, which is generally described by a normal distribution. The α particles must traverse more than twice the target thickness before they appear in the spectrum at C_{2O}. The detector resolution, energy straggling, and multiple scattering may contribute to the width of the step at C_{2O}. In the present experimental conditions, the fluctuation in α-particle energy from energy straggling, in addition to a small uncertainty in the scattering angles caused by multiple scattering, is approximately Gaussian. As one can demonstrate by folding a step function with Gaussian distribution functions, the position of the original step is actually well approximated by that of the midpoint obtained in the manner illustrated in Figure 1. The energies corresponding to channel numbers C_{2B} and C_{2O} therefore are given, respectively, by the previously defined E_{2B} and E_{2O}. The energy at any other channel in the spectrum can be determined by examining the

TABLE I. Experimental details.

Element[a]	Evaporation technique[b]	Target backing	Number of targets	Target thickness ($\mu g/cm^2$) range	average	Number of data points	Stopping power (10^{-15} eV cm^2) Average[c]	Error[d]
Se	Ta boat	Ta or Al	7	52–317	165	86	82.5	± 2.70
Y	W or Ta boat	Ta or Al	6	45–154	85	73	107.7	± 2.67
Zr	Electron beam rf sputtering	Ta or Al	6	52–224	128	86	113.8	± 2.81
Nb	Electron beam	Ta or Al	4	55–185	103	64	116.0	± 2.84
Mo	Electron beam rf sputtering	Ta or Al	7	34–218	124	88	109.1	± 2.41
Sb	Ta boat	Ta or Al	6	74–136	106	96	113.4	± 2.91
Te	Ta boat	Ta or al	8	81–208	142	116	117.4	± 2.55
La	Ta boat	Al	5	63–255	147	68	141.3	± 3.93
Dy	Ta boat	Al	4	111–239	172	72	119.5	± 3.21
Ta	rf sputtering	Al	3	148–299	199	50	113.0	± 2.42
W	rf sputtering	Al	4	156–351	252	44	110.9	± 2.36
Au	Al_2O_3-coated Mo boat	Al	5	128–190	157	77	120.4	± 2.56

[a]Purity > 99.5%.

[b]Specific boat for evaporation by resistance heating is given. A carbon crucible was used for electron-beam bombardment. rf sputtering was kindly carried out by R. Gooch.

[c]Average over $0.3 \leq E_\alpha \leq 2.0$ MeV.

[d]Mainly derived from rms deviation of the data to a fitted smooth curve.

similar energy spectra taken at different bombarding energies. However, in order to have a reasonable separation between C_{2B} and C_{2O}, large amplification was required, and one had to change the bias level of the biased amplifier from the run taken at one value of E_α to another. To ensure that no extra nonlinearity was introduced by so doing, and to facilitate the data reduction, three pulses of different voltage from a precision pulser were fed in through the preamplifier and were analyzed every time after a spectrum was taken. The voltage V_{2B} corresponding to channel C_{2B} and the voltage per channel dV/dC were computed. The energy per voltage reading dE/dV still would have to be found from the $E_{2B} - V_{2B}$ correspondence established from several runs at neighboring bombarding energies. This procedure of obtaining the energy per channel $dE/dC = (dE/dV)(dV/dC)$ takes into account the effect due to the energy variation of the stopping cross section in the dead layer on the surface of the counter. The quantity $\Delta E = E_{2B} - E_{2O} = (dE/dC)(C_{2B} - C_{2O})$, which is important for deriving the stopping cross section, was then calculated.

To prevent La or Dy from oxidation, an aluminum layer of approximately 15 $\mu g/cm^2$ was evaporated on top of this chemically reactive target film, which has already been prepared on a thick Al backing. Because an α particle has to go through this pro-

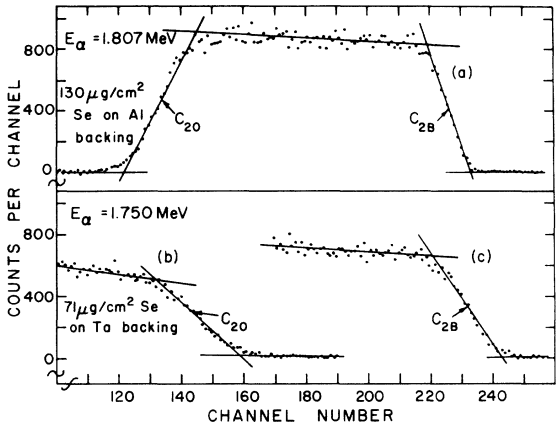

FIG. 1. Energy spectra of α particles elastically scattered at $\theta = 130°$. The target orientation was so fixed that the directions along both incident and detected α particles were 25° with respect to the normal to the target surface. Spectrum (a) describes α-particle scattering by a selenium target film prepared on an Al backing. The channel numbers C_{2B} and C_{2O}, i.e., the midpoints of the indicated steps, correspond to scattering from the front and back surfaces of the target film, respectively. Spectra (b) and (c) were taken at the bombarding energy $E_\alpha = 1.750$ MeV; they represent scattering from a clean Ta blank and from another onto which selenium has been uniformly deposited. In this case, however, both C_{2B} and C_{2O} correspond to scattering by Ta atoms on the front surfaces of the respective blanks.

tecting layer twice before it gets detected, the energy E'_{2B} corresponding to channel number C_{2B} is now not exactly equal to kE_α. For calibration purposes, elastic α-particle energy spectra from a clean Ta blank were also taken. The energy per channel dE/dC and therefore E'_{2B} were determined using the similar procedure just described. Since the difference between kE_α and E'_{2B} is proportional to the energy loss of α particles in the Al layer, the layer thickness was obtained from a least-squares fit of the quantities $(kE_\alpha - E'_{2B})$ to the known stopping cross section of α particles in Al.[6] From this thickness, E_{2B} and ΔE, corresponding to the case of no such Al layer, can be calculated.

For all the targets, the second terms in Eqs. (1) and (2) amount to corrections less than 2% and 10 keV in $S_e(E_x)$ and E_x, respectively. S_e and E_x were computed by neglecting these terms and were then fitted to a smooth curve (e.g., a polynomial of the third degree), describing S_e as a function of E_x. The quantities $S_e(E_\alpha)$, $S_e(E_{2O})$, and d^2S_e/dE_x^2, evaluated from the smooth curve, were substituted into the equations to deduce the final values for S_e and E_x. The experimental error or spread shown in Table I was assigned mainly from the rms deviation of the data points from the smooth curve. The deviations obtained for elements Nb, Dy, and Ta happened to be relatively small; they were suitably increased to values that are comparable with those for other elements, which are similar in method of target preparation. In Fig. 2 the resulting stopping cross sections are plotted as a function of α-particle energy.

III. DATA ANALYSIS

In the low-velocity region for which the incident-particle velocity v is much smaller than those of the target atomic electrons, i.e., $v \ll Z_2e^2/\hbar$, it has been found that the stopping cross section S_e can be satisfactorily described by $S_e = cv$. This velocity dependence of S_e has been predicted by Fermi and Teller[13] and Lindhard *et al.*[14] from considering the energy loss of charged particles in an electron gas, and by Firsov[15] from interpreting S_e as resulting from the deceleration of the particle due to electron-flux exchange. Firsov's method has been widely used to calculate the constant of proportionality c, using an electronic charge density derived from more realistic atomic wave functions. These calculations have proved[1] very suc-

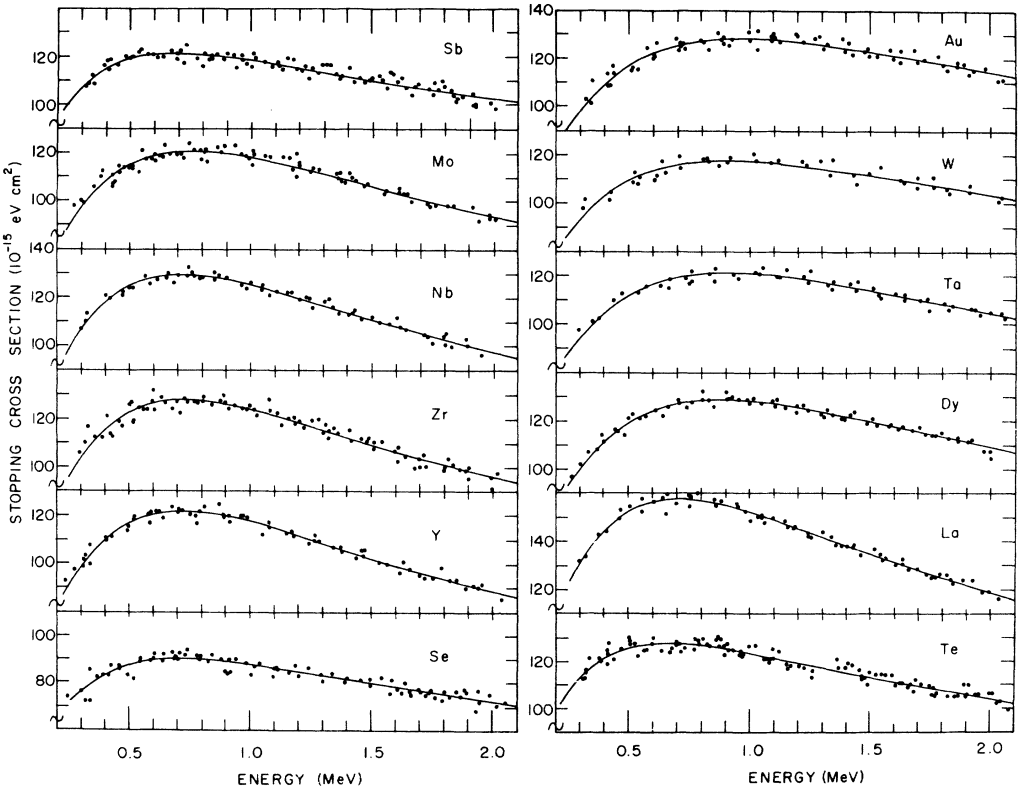

FIG. 2. Stopping cross sections of α particles vs energy in Se, Y, Zr, Nb, Mo, Sb, Te, La, Dy, Ta, W, and Au. The experimental error ranges from ± 2.2 to 3.3% of the average stopping cross section for the corresponding element. The solid curves were calculated from Brice's formula using the parameters tabulated in Table II. For each element, these parameters were obtained individually by a least-squares fit of the data to the formula.

cessful in describing the Z_1 oscillations of S_e observed at low energies. In the high-velocity region ($v \gg Z_2 e^2/\hbar$), on the other hand, S_e is known to follow the Bethe formula.[16] Any analytic expression for S_e, which has the above-mentioned behavior in the low- and high-velocity regions, could be compared with the experimental results and be used to predict S_e in velocity regions for which no measurement has been made. As will be discussed, the formula given by Brice,[11] i.e.,

$$S = \frac{4\hbar^2}{5m}\left(\frac{Z_1 + Z_2}{1+(av/v_0)^n}\right) \times \left[\epsilon^{1/2}\left(\frac{30\epsilon^2+53\epsilon+21}{3(\epsilon+1)^2}\right) + (10\epsilon+1)\tan^{-1}\epsilon^{1/2}\right], \quad (3)$$

with $\epsilon = (v/2v_0 z)^2$ and $v_0 = e^2/\hbar$, has approximately the above-mentioned velocity dependence. This expression contains three parameters, n, a, and z, and has been obtained using Firsov's method. The electron flux, however, is computed from a quantum-mechanical definition using $1s$ hydrogenic wave functions. Although, as Brice has indicated, the basic physical arguments which have gone into the derivation are relatively crude, and certainly are not correct in the high-velocity region, expression (3) has been shown to agree with experimental results covering a considerably large velocity region, at least for stopping cross sections measured in many gaseous media.

The energy dependence of S_e measured in this work was examined by a least-squares fit of the experimental data points to expression (3). For each target element, let the stopping cross section measured at $E_\alpha = E_j$ be Y_j; the parameters n, a, and z were determined by minimizing the quantity

$$F = \frac{1}{\sigma^2}\sum_{j=1}^{J}[Y_j - S(E_j)]^2. \quad (4)$$

For a set of trial values of the parameters, $S(E_j)$ is evaluated from expression (3). J, the total number of data points, and σ^2, the square of the corresponding error assigned, are tabulated in Table I. Since it is relatively easy to compute the partial derivatives of S with respect to the parameters, the right-hand side of Eq. (4) was first linearized.[17] The solution from minimization was iterated until it became stationary. The error matrix[18] D was then calculated by inverting a matrix, directly constructed from the second partial derivatives of F with respect to the parameters at the final solution. Table II lists the parameters corresponding to this solution and the matrix elements of D. Stopping cross sections calculated from these parameters are shown in Table III and Fig. 2. Because the fits turned out to be extremely good, it was tempting to extend the calculation to energies other than $0.3 \le E_\alpha \le 2.0$ MeV.

The statistical error ΔS in S can be computed from the relation[18]

$$(\Delta S)^2 = \left(\frac{\partial S}{\partial n}\right)^2 D_{nn} + \left(\frac{\partial S}{\partial a}\right)^2 D_{aa} + \left(\frac{\partial S}{\partial z}\right)^2 D_{zz} + 2\left[\left(\frac{\partial S}{\partial n}\right)\left(\frac{\partial S}{\partial a}\right) D_{na} + \left(\frac{\partial S}{\partial n}\right)\left(\frac{\partial S}{\partial z}\right) D_{nz} + \left(\frac{\partial S}{\partial a}\right)\left(\frac{\partial S}{\partial z}\right) D_{az}\right], \quad (5)$$

and it is expected that $\Delta S/S$ increases as the energy moves farther away from the measured energy region. At $E_\alpha = 0.128$ and 8.0 MeV, for instance, the quantities $\Delta S/S$ were found to be less than 3% and 7%, respectively, for all the elements. Figure 3 shows the stopping cross sections in elements Se, Ta, and Au for $0.1 \le E_\alpha \le 10$ MeV. The stopping cross sections represented by the dashed curves were calculated at energies outside the measured energy region. In this extrapolation, a possible error other than the statistical one can occur due to the possibility that Brice's formula given by

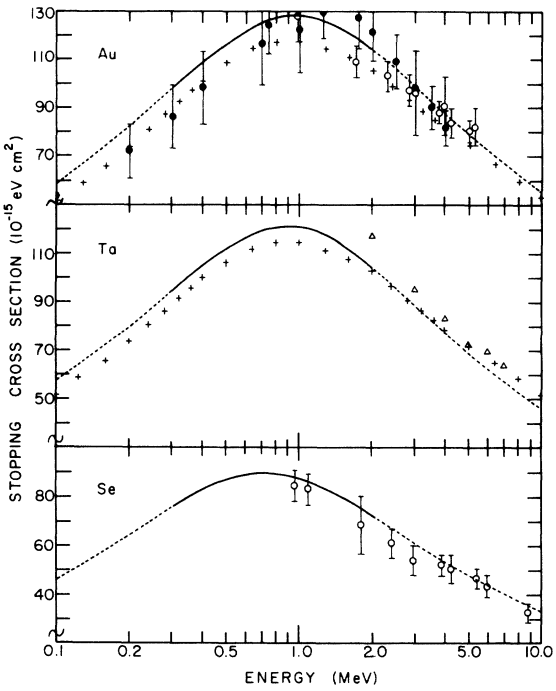

FIG. 3. Stopping cross sections of α particles in Se, Ta, and Au for $0.1 \le E_\alpha \le 10$ MeV. The dashed curves, extrapolated from their corresponding solid curves (also shown in Fig. 2), were calculated from Brice's formula using the same parameters extracted from the least-squares fits. The results from Whaling (Ref. 3), Nakata (Ref. 19), Leminen (Ref. 1, where proper scaling was made to the original proton stopping cross sections), and Northcliffe and Schilling (Ref. 20) are included for comparison. They are given by closed circles, open circles, triangles, and crosses, respectively.

TABLE II. Summary of the parameters and error matrix obtained from the least-squares fits of the experimental data to Brice's formula.

Element	n	a	z	Error matrix[a] (10^{-4}) D_{nn}	D_{aa}	D_{zz}	D_{na}	D_{nz}	D_{az}
Se	3.10	0.386	2.00	41.2	1.01	23.1	−6.12	28.1	−4.80
Y	3.51	0.361	1.93	23.4	0.189	5.07	−1.92	9.34	−0.964
Zr	3.40	0.368	1.87	87.2	1.07	24.8	−9.49	45.1	−5.13
Nb	3.33	0.376	1.83	26.6	0.384	8.46	−2.94	13.0	−1.78
Mo	3.35	0.359	2.03	27.6	0.287	8.21	−2.67	13.8	−1.52
Sb	2.81	0.431	1.90	38.9	2.94	46.7	−10.4	40.7	−11.7
Te	2.90	0.426	1.88	9.25	0.526	8.81	−2.06	8.02	−2.14
La	3.34	0.371	2.00	29.4	0.433	12.4	−3.24	16.2	−2.29
Dy	3.19	0.324	2.85	56.9	0.429	30.7	−4.60	37.6	−3.60
Ta	3.13	0.315	3.26	69.6	0.537	56.0	−5.76	57.4	−5.46
W	3.01	0.321	3.28	59.1	0.587	55.6	−5.51	52.3	−5.68
Au	3.05	0.308	3.38	54.3	0.356	38.9	−4.17	43.0	−3.71

[a]Symmetric, i.e., $D_{an}=D_{na}$, $D_{zn}=D_{nz}$, and $D_{za}=D_{az}$.

expression (3) might not be accurate in some particular energy region. As can be shown easily, the stopping cross section from expression (3) becomes proportional to v in the low-velocity region. Since the low-velocity stopping cross section can be satisfactorily described by $S_e=cv$, as mentioned earlier, one would expect a small error in the extrapolation for the energy region $0.1 \leq E_\alpha \leq 0.3$ MeV. For $2.0 \leq E_\alpha \leq 10$ MeV, the curves shown in Fig. 3 agree reasonably well with other results,[3,19–21] indicating that the extrapolation in this energy interval is acceptable, at least for the elements Se, Ta, and Au.

For other elements there are practically no stopping cross sections available to compare with the extrapolation. In order to illustrate the usefulness of expression (3) for the elements in general, extrapolated stopping cross sections were compared with the Bethe formula,

$$S' = \frac{4\pi Z_1^2 e^4}{m v_0^2} \frac{1}{\chi} [\ln\chi + \ln(2mv_0^2 Z_2/I)] , \qquad (6)$$

expressed in terms of an energy variable $\chi = v^2/Z_2 v_0^2$. For high velocities, S of expression (3) varies as v^{2-n}, a power-law dependence. Because S' can be approximated by a power-law dependence only for a fixed finite energy interval, it is not surprising to find that the mean excitation energy per electron I/Z_2, obtained by equating S and S', depends on the choice of χ. The values of χ at the matching points, however, can be fixed by further requiring that the slopes of S and S' at χ also agree, and were found, except for elements Sb and Te, to correspond to the α-particle energies greater than 8.0 MeV. The I/Z_2 estimated from these matching points are 12.6 ± 1.4, 16.9 ± 3.2, 17.3 ± 8.6, 12.6 ± 2.6, 15.8 ± 3.7, 7.7 ± 0.4, 8.0 ± 0.3, 14.4 ± 3.7, 13.2 ± 3.4, 14.8 ± 3.6, 11.6 ± 1.7, and 10.6 ± 1.9 eV, respectively, for elements Se, Y, Zr, Nb, Mo, Sb, Te, La, Dy, Ta, W, and Au. The errors were merely computed from relation (5), and therefore include the statistical errors only. Surprisingly, the values for I/Z_2 turn out to be quite comparable with those cal-

TABLE III. Stopping cross sections for α particles.[a]

Energy (MeV)	Se (3.3%)	Y (2.5%)	Zr (2.5%)	Nb (2.4%)	Mo (2.5%)	Sb (2.6%)
0.3	76.2	98.6	103.8	106.8	97.3	107.3
0.4	83.2	110.0	115.4	118.1	108.2	115.0
0.5	87.3	116.8	122.4	124.8	115.0	119.1
0.6	89.4	120.4	126.0	128.2	118.7	121.0
0.7	90.0	121.6	127.2	129.2	120.3	121.4
0.8	89.8	121.1	126.8	128.7	120.4	121.0
0.9	89.0	119.5	125.4	127.2	119.5	120.0
1.0	87.8	117.3	123.2	125.1	117.8	118.7
1.1	86.4	114.6	120.7	122.5	115.8	117.2
1.2	84.9	111.6	117.9	119.8	113.4	115.6
1.3	83.3	108.6	114.9	116.9	110.9	113.9
1.4	81.6	105.5	112.0	114.0	108.4	112.2
1.5	80.0	102.5	109.1	111.2	105.8	110.5
1.6	78.4	99.6	106.2	108.4	103.3	108.9
1.7	76.8	96.7	103.4	105.7	100.8	107.2
1.8	75.3	93.9	100.7	103.0	98.4	105.7
1.9	73.8	91.3	98.2	100.5	96.1	104.2
2.0	72.4	88.8	95.7	98.1	93.8	102.7
Energy (MeV)	Te (2.2%)	La (2.8%)	Dy (2.7%)	Ta (2.2%)	W (2.2%)	Au (2.2%)
0.3	113.0	131.1	100.2	94.5	93.3	98.0
0.4	121.3	114.7	111.5	104.8	102.9	108.8
0.5	125.5	152.6	119.0	111.8	109.4	116.4
0.6	127.2	156.5	123.9	116.3	113.6	121.5
0.7	127.3	157.7	126.7	119.1	116.1	124.8
0.8	126.5	156.9	128.1	120.5	117.4	126.7
0.9	125.1	155.0	128.4	120.9	117.8	127.6
1.0	123.4	152.3	127.9	120.6	117.6	127.8
1.1	121.5	149.2	126.8	119.8	116.9	127.4
1.2	119.4	145.7	125.4	118.6	115.9	126.6
1.3	117.3	142.2	123.7	117.1	114.7	125.4
1.4	115.3	138.6	121.8	115.5	113.3	124.1
1.5	113.2	135.1	119.8	113.8	111.8	122.6
1.6	111.2	131.7	117.7	112.0	110.3	121.1
1.7	109.3	128.3	115.6	110.1	108.7	119.4
1.8	107.4	125.1	113.5	108.3	107.1	117.7
1.9	105.6	122.0	111.5	106.4	105.5	116.1
2.0	103.9	119.0	109.5	104.6	103.9	114.4

[a]Stopping cross sections are given in units of 10^{-15} eV cm^2. The numbers in parentheses under the elements are the averaged percentage error.

culated by Chu and Powers[22] and those for Ta and W recommended by Bichsel.[23] For Sb and Te both the value and the slope of S match those of S' at α-particle energies 3.2 and 5.0 MeV, respectively. Since it is not clear whether the inner-shell corrections to expression (6) could be neglected at these low energies, in spite of the small statistical errors, the estimated I/Z_2 for these two elements may not be as good as for the others.

For all the elements studied, it was generally observed that S becomes systematically higher than S' when χ reaches values greater than that of the matching point. The size of this discrepancy should be estimated, using some reasonable value for I/Z_2, before one decides to take the stopping cross section, extrapolated from Brice's formula at high energy. The limitation, as mentioned earlier, is due to the difficulty that one cannot approximate the Bethe formula by a simple power-law dependence over too wide an energy interval.

IV. DISCUSSION

The quantum-mechanical theory of energy loss was developed by Bethe[16] around 1930. It works successfully in the velocity region for which $v \gg Z_2 e^2/\hbar$. The mean excitation energy I is the only parameter needed to characterize the Bethe formula. The problem, however, becomes very involved when one tries to estimate I or to extend the formula to the lower-velocity region by applying the inner-shell corrections. As has been shown by Lindhard and Schaff,[24] the statistical method they developed can give a fairly accurate description of the energy-loss phenomena. Along this direction, Rousseau, Chu, and Powers[7,8] have calculated the α-particle stopping cross sections for all the elements throughout the periodic table. Their results are shown for $E_\alpha = 0.8$ and 2.0 MeV in Fig. 4. In addition to the data obtained in this work for 12 elements, data for Si and Ge,[25] for Be, C, Mg, Al, Ti, V, Cr, Mn, Fe, Co, Ni, Cu, Pd, Ag, In, and Sn,[6] for He, Ne, Kr, and Xe,[10] for H, N, and O,[26] and for F, Cl, Br, and I[27] are included in the figure for comparison. The positions of extrema in the oscillatory Z_1 dependence of S_e appear to be identical to those found in the Z_2 dependence. The minima at atomic numbers 11, 30, 46, 50, and 79 occur for those elements having closed or almost closed shells, while the maxima at 8, 22, and 41 correspond to elements whose $2p$, [$4s$, $3d$], and [$5s$, $4d$] shells, respectively, are about half-filled. The maxima found at 57 and predicted at 90 have different characteristics, and are interesting because the elements following them are beginning to fill the $4f$ and $5f$ subshells. Considering the degenerate [$6s$, $4f$, $5d$] or [$7s$, $5f$, $6d$] as a shell, the shells for elements 57 and 90, however, are by no means close to half-filled. The experimental-theoretical agreement in the periodic dependence of S_e on Z_2 shown in Fig. 4 is indicative that the statistical approach is actually quite effective. Further support for this approach has also been reported by Chu and Powers,[22] who have calculated the mean excitation energies for all elements. The calculated I/Z_2 versus Z_2 reveals structure observed in many experiments.

Lindhard's statistical approach starts from a well-established result from plasma theory, namely, the energy loss of charged particles in a uniform electron gas. As Fano[28] has pointed out, a difficulty was encountered when this result is applied to atomic electrons. The plasma theory assumes that the average electron density is nearly constant over a wavelength of the plasma oscillation, a condition which is not verified in the interior of atoms. However, it is believed that the series of systematic measurements of α-particle stopping cross sections, of which this work constitutes a part, would be helpful to understand why the method works.

We have shown that it is possible to parametrize the measured α-particle stopping cross sections by three parameters using Brice's formula. These parameters, from the error matrix obtained in the

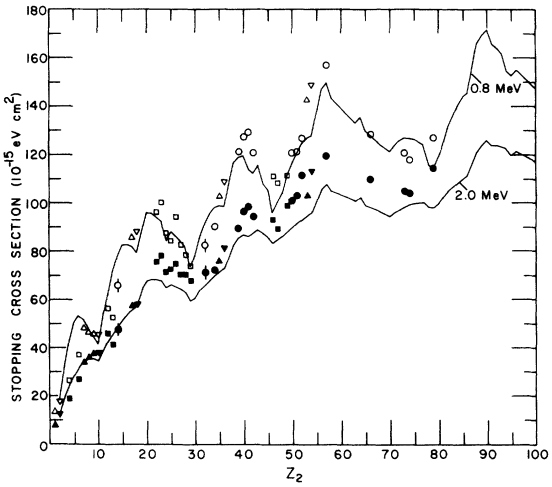

FIG. 4. α-particle stopping cross section vs the stopping-element atomic number Z_2 at 0.8 and 2.0 MeV. The solid curves are taken from the calculations based on Lindhard's statistical approach, carried out by Rousseau, Chu, and Powers (Refs. 7 and 8). Open and closed symbols, respectively, correspond to the 0.8- and 2.0-MeV data. The stopping cross sections S_e measured in this work are given by circles. The S_e, measured in other solid elements and represented by circles with bars and squares, respectively, are taken from Refs. 25 and 6. Those from normal gases (Ref. 10) are given by inverted triangles. Finally, the triangles represent the S_e derived from the molecular stopping-cross-section measurements of Refs. 26 and 27.

least-squares fit, were found not to be independent. It still would be interesting to carry out a systematic survey on the Z_2 dependence of the three parameters for more elements, and to see how the parameters are related to the electronic properties of the stopping atom. The stopping cross sections calculated from Brice's formula were found to be acceptable for those α-particle energies which were not very much greater than the energy at which both the values and slopes of the stopping cross sections given by Brice's formula and Bethe's formula matched. For higher energies the former was found to deviate from the latter. Therefore one could not really say that Brice's formula generally gives quite accurate stopping cross sections for incident energies up to 10 MeV/amu, as suggested by Brice.

ACKNOWLEDGMENTS

We are happy to acknowledge the assistance of A. S. Lodhi and G. Hoffman in carrying out this experiment, and are also grateful to Dr. W. K. Chu and to Dr. H. L. Cox for their helpful discussions.

---

*Research supported in part by the National Science Foundation.

[1]I. M. Cheshire and J. M. Poate, in *Atomic Collision Phenomena in Solids*, edited by O. W. Palmer, M. W. Thompson, and P. D. Townsend (North-Holland, Amsterdam, 1970), p. 351.

[2]J. Bøttinger and F. Bason, Radiat. Eff. 2, 105 (1970).

[3]W. Whaling, in *Handbuch der Physik*, edited by S. Flügge (Springer-Verlag, Berlin, 1958), Vol. 34, p. 193.

[4]K. R. MacKenzie, in Natl. Acad. Sci.-Natl. Res. Council, Publ. No. 753, Sec. I-2, 1960 (unpublished).

[5]W. White and R. M. Mueller, Phys. Rev. 187, 499 (1969).

[6]W. K. Chu and D. Powers, Phys. Rev. 187, 478 (1969).

[7]C. C. Rousseau, W. K. Chu, and D. Powers, Phys. Rev. A 4, 1066 (1971).

[8]W. K. Chu and D. Powers, Phys. Lett. A 38, 267 (1972).

[9]For α particles in the stopping elements studied in this work, the energy loss due to the nuclear collisions was estimated, using the results given in Ref. 14, to be less than 2.5% of the loss due to the electronic collisions, if the α-particle energy is greater than or equal to 0.1 MeV.

[10]W. K. Chu and D. Powers, Phys. Rev. B 4, 10 (1971).

[11]D. K. Brice, Phys. Rev. A 6, 1791 (1972).

[12]D. Powers, W. K. Chu, and P. D. Bourland, Phys. Rev. 165, 376 (1968).

[13]E. Fermi and E. Teller, Phys. Rev. 72, 399 (1947).

[14]J. Lindhard, M. Scharff, and H. E. Schiött, K. Dan. Vidensk. Selsk. Mat.-Fys. Medd. 33, No. 14 (1963).

[15]O. B. Firsov, Zh. Eksp. Teor. Fiz. 36, 1517 (1962) [Sov. Phys.-JETP 9, 1076 (1959)].

[16]H. A. Bethe and J. Ashkin, in *Experimental Nuclear Physics*, edited by E. Segrè (Wiley, New York, 1953), Vol. I, p. 166.

[17]B. M. Shchigolev, in *Mathematical Analysis of Observations* (American Elsevier, New York, 1965), pp. 243–247.

[18]J. Orear, University of California Radiation Laboratory Report No. UCRL-8417, 1958 (unpublished).

[19]H. Nakata, Can. J. Phys. 47, 2545 (1969).

[20]L. C. Northcliffe and R. F. Schilling, Nucl. Data A 7, 233 (1970).

[21]E. Leminen, Ann. Acad. Sci. Fenn. Series A6 386, 1 (1972).

[22]W. K. Chu and D. Powers, Phys. Lett. A 40, 23 (1972).

[23]H. Bichsel, in *Radiation Dosimetry*, edited by F. H. Attix and W. C. Roesch (Academic, New York, 1968), Vol. I, p. 157.

[24]J. Lindhard and M. Scharff, in Ref. 4. Sec. II-1.

[25]W. K. Lin, H. G. Olson, and D. Powers, J. Appl. Phys. (to be published).

[26]P. D. Bourland, W. K. Chu, and D. Powers, Phys. Rev. B 3, 3625 (1971).

[27]D. Powers, W. K. Chu, R. J. Robinson, and A. S. Lodhi, Phys. Rev. A 6, 1425 (1972).

[28]U. Fano, in Ref. 4, Appendix.